Inorganic Chemistry

Communication

pubs.acs.org/IC

Electronic Structural Changes of Mn in the Oxygen-Evolving Complex of Photosystem II during the Catalytic Cycle

Pieter Glatzel,*[,†] Henning Schroeder,[‡,∞] Yulia Pushkar,[‡,§] Thaddeus Boron, III,[⊥] Shreya Mukherjee,[∥] George Christou,[∥] Vincent L. Pecoraro,[⊥] Johannes Messinger,[¶] Vittal K. Yachandra,*[,‡] Uwe Bergmann,*[,▽] and Junko Yano*[,‡]

[†]European Synchrotron Radiation Facility, 38000 Grenoble, France

[‡]Physical Biosciences Division, Lawrence Berkeley National Laboratory, Berkeley, California 94720, United States

[⊥]Department of Chemistry, University of Michigan, Ann Arbor, Michigan 48109, United States

[∥]Department of Chemistry, University of Florida, Gainesville, Florida 32605, United States

[¶]Institutionen för Kemi, Kemiskt Biologiskt Centrum, Umeå Universitet, Umeå, Sweden

[▽]LCLS, SLAC National Accelerator Laboratory, Menlo Park, California 94025, United States

Supporting Information

ABSTRACT: The oxygen-evolving complex (OEC) in photosystem II (PS II) was studied in the S_0 through S_3 states using 1s2p resonant inelastic X-ray scattering spectroscopy. The spectral changes of the OEC during the *S*-state transitions are subtle, indicating that the electrons are strongly delocalized throughout the cluster. The result suggests that, in addition to the Mn ions, ligands are also playing an important role in the redox reactions. A series of Mn^{IV} coordination complexes were compared, particularly with the PS II S_3 state spectrum to understand its oxidation state. We find strong variations of the electronic structure within the series of Mn^{IV} model systems. The spectrum of the S_3 state best resembles those of the Mn^{IV} complexes $Mn_3^{IV}Ca_2$ and saplnMn$_2^{IV}$(OH)$_2$. The current result emphasizes that the assignment of formal oxidation states alone is not sufficient for understanding the detailed electronic structural changes that govern the catalytic reaction in the OEC.

The oxygen-evolving complex (OEC) located in the photosystem II (PS II) membrane-bound protein in plants, algae, and cyanobacteria catalyzes the water-oxidation reaction.[1] The OEC, an oxo-bridged complex of four Mn and one Ca ions (Mn_4CaO_5 cluster), couples the four-electron chemistry of water oxidation with the one-electron photochemistry of the reaction center by sequentially storing oxidizing equivalents through five intermediate *S* states (S_i, i = 0−4), before one molecule of dioxygen is evolved. The Mn_4CaO_5 cluster provides a high degree of redox and chemical flexibility so that several oxidizing equivalents can be stored during the *S*-state cycle. To understand the mechanism of water oxidation in detail, it is crucial to understand the changes of the electronic structure in the OEC over the whole course of the catalytic cycle.[2]

There is a consensus that Mn-centered oxidation occurs during the S_0 to S_1 and S_1 to S_2 transitions. However, there has been a long debate regarding the nature of the S_2 to S_3 transition. Within the context of localized oxidation, the formal oxidation state of the native S_1 state has been assigned to $Mn_2^{III}Mn_2^{IV}$ and S_2 to $Mn^{III}Mn_3^{IV}$. In the S_0 state, involvement of Mn^{II} has been discussed, while recent ENDOR studies[3] support the formal oxidation state of $Mn_3^{III}Mn^{IV}$. In the S_3 state, the question remains whether a Mn-centered oxidation occurs[4] and therefore all Mn atoms become Mn^{IV}, or a ligand-centered oxidation takes place before O−O bond formation and release of molecular oxygen.[5] This incomplete understanding of the S_2 to S_3 transition has led to two different types of proposed O_2 evolution mechanisms; one incorporating the nucleophilic attack of high-valent Mn and the other involving oxo radicals.[2,6] Fundamental differences in the chemistry of O−O bond formation and O_2 evolution exist between the two types of mechanisms.

In our earlier resonant inelastic X-ray scattering (RIXS) study, it was shown that the electron in the S_1 to S_2 transition is removed from a strongly delocalized orbital, indicating strong covalency within the Mn_4CaO_5 cluster and that the oxidation therefore cannot be assigned to just one Mn atom in the OEC.[7] In the current study, we present RIXS data on PS II from S_0 through S_3 states of the OEC. We compared the S_3 spectrum with model compounds, where Mn has the formal oxidation state IV, with different nuclearities, types of ligands, and geometries.

In 1s2p RIXS spectroscopy (Scheme S1 in SI), a Mn 1s electron is excited into the lowest unoccupied molecular orbitals (LUMOs). The orbitals have mainly Mn 3d character mixed with Mn 4p and ligand orbitals. The electronic configuration can be approximated by $1s^1 3d^{n+1}$, and the spectral features are the K absorption preedge. The excited states decay and release a photon whose energy is recorded in order to obtain the energy retained (energy transfer). The most probable transition is 2p to 1s to reach the final state configuration $2p^5 3d^{n+1}$, which is formally identical with that of L-edge spectroscopy.

RIXS spectra are shown as a two-dimensional contour plots (*c.f.* Figure 1) with incident energy and energy transfer along the axes. The spectral broadening along the energy transfer axis is not

Received: March 10, 2013
Published: May 6, 2013

   dx.doi.org/10.1021/ic4005938 | *Inorg. Chem.* 2013, 52, 5642−5644

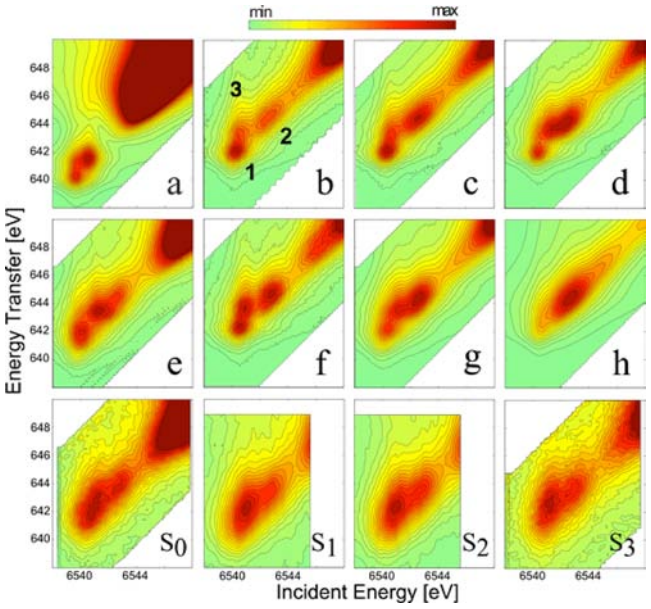

Figure 1. Contour plots of Mn 1s2p RIXS planes of model compounds and the OEC in PS II in the S_0 to S_3 states: (a) $Mn^{II}O$; (b) $salpn_2Mn^{IV}{}_2(OH)_2$; (c) $salpn_2Mn^{IV}{}_2(O)(OH)$; (d) $salpn_2Mn^{IV}{}_2(O)_2$; (e) $phen_4Mn^{IV}{}_2(O)_2$; (f) $Mn^{IV}{}_3Ca_2$; (g) $Mn^{IV}{}_3(O)_4$Acbpy; (h) $Mn^{IV}(O)_2$. The energy axes are identical for all spectra. The intensity is normalized to the maximum in the preedge region for all spectra.

governed by the short core hole lifetime of the intermediate state, but the longer lived final state, resulting in sharp spectral features.

Figure 1 shows RIXS spectra of PS II in the S_0 to S_3 states and a series of Mn model complexes. The 1s2p RIXS planes of Mn^{IV} systems (Figure 1b–h; chemical structures of parts b–g are shown in the Supporting Information, SI) vary significantly, demonstrating that a Mn^{IV} species does not provide a single unique spectroscopic fingerprint. The spectral shape is strongly influenced by the local density of unoccupied electronic states. The K absorption preedges obtain spectral intensity from electric dipole and quadrupole transitions depending on the local symmetry. Therefore, the spectral intensity may vary considerably depending on the number and type of ligands.[8] The coordination complexes in Figure 1 all have six-coordinated Mn, and the ratio between the dipole and quadrupole contributions to the preedge will vary little. We attribute intensity variations to modifications in the composition of the molecular orbitals.

The overall trend observed in the 1s2p RIXS planes is a shift of the spectral intensity to higher energies with increasing positive charge on the metal. The solid-state system $Mn^{IV}O_2$ (Figure 1h) has its highest energy peak at 6542.9 eV, representing the most ionic form of Mn^{IV} possibly induced by the extended structure of the Mn–O lattice. The Mn^{IV} coordination complexes (Figure 1b–g)[9] are distinctly different from the oxides. They show three main spectral features in the energy range of 6539–6544 eV. The low-energy feature at 6541 eV (indicated as 1 in Figure 1b) is sharper than the structures at higher energies. It corresponds to the excitation of the 1s electron into LUMOs that are localized and therefore exhibit a more atomic character. The effect of the ligand environment becomes more dominant toward higher energies (6541–6544 eV, indicated as 2 in Figure 1b), resulting in broader spectral features due to the orbital splittings. The intensity around 6542 eV appears to be off-diagonal (indicated as 3 in Figure 1b), shifted toward higher energy transfer, which is caused by strong (2p,3d) electron–electron interactions.

A series of di-μ-oxo-bridged Mn-salpn compounds ($salpn_2Mn^{IV}{}_2(OH)_2$, $salpn_2Mn^{IV}{}_2OOH$, and $salpn_2Mn^{IV}{}_2O_2$; Figure 1b–d) demonstrates the sensitivity of 1s2p RIXS to the sequential protonation of the bridging oxygen. They show a transfer of the spectral intensity from low to high energy features. Replacing OH^- with O^{2-} thus results in a 1s2p RIXS plane with the spectral weight predominantly in the region where also $Mn^{IV}O_2$ (Figure 1h) shows its strongest spectral feature.

The spectra of $Mn_3{}^{IV}O_4$Acbpy (Figure 1g), $salpn_2Mn^{IV}{}_2O_2$ (Figure 1d), and $phen_4Mn^{IV}{}_2O_2$ (Figure 1e) show maximum intensity at higher energies (6541–6544 eV), as opposed to other compounds (e.g., Figure 1b,f). In all cases, the di-μ-oxo bridge is not protonated. This confirms that the bridging ligand including its degree of protonation has a strong influence on the electronic structure around Mn. The subtle differences at higher energies observed among the three compounds reflect the orbital modifications at the Mn sites when replacing N with O (SI, Figure S1) and slightly changing the bond distances and angles. $Mn_3{}^{IV}O_4$Acbpy (Figure 1g) with two di-μ-oxo bridges and additional O ligands have their main peak intensity at higher energy. The $phen_4Mn^{IV}{}_2O_2$ complex (Figure 1e) with N ligands and two di-μ-oxo bridges, by contrast, shows spectral intensity at lower energies than $salpn_2Mn^{IV}{}_2O_2$ (Figure 1d), where each Mn has two additional O ligands. The spectrum of Mn_3Ca_2 (Figure 1f) resembles that of $salpn_2Mn^{IV}{}_2(O)(OH)$ with single protonation of the oxo bridge (Figure 1c). The Mn_3Ca_2 compound contains a cubane-like structure that consists of a $Mn_3{}^{IV}CaO_4$ moiety. The presence of Ca within the cubane-like structure appears to modify the electronic structure of Mn in a way similar to what we observe for protonation of the oxo bridge.

Pure S_0, S_1, S_2, and S_3 spectra shown in Figures 1 and 2 were obtained by deconvolution of the flash-illuminated samples using

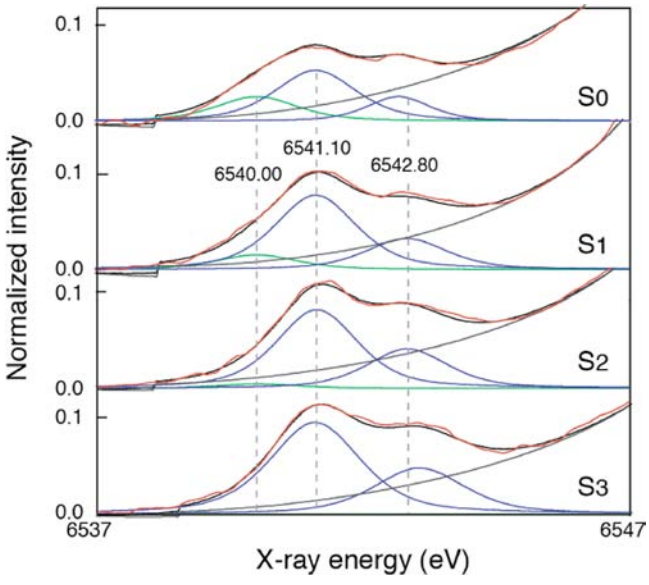

Figure 2. K absorption preedges and fit of Mn in PS II (red, experimental data; black, fit; blue and green, peak components; gray, background). The dashed lines are guides to the eye.

the calculated S-state distribution from electron paramagnetic resonance (EPR; see the SI, Figure S2a–c). Within the series of PS II data, we observe a small shift of the spectral intensity to higher energies between S_0 and S_3, confirming oxidation at the Mn sites during the catalytic cycle.[7] This is also observed in the XAS preedge spectra, as shown in Figure 2. A low-energy

dx.doi.org/10.1021/ic4005938 | Inorg. Chem. 2013, 52, 5642–5644

shoulder appears in the S_0 preedge spectrum, which is seen as a low-energy component in the RIXS S_0 spectrum (Figure 1). Upon the S_0 to S_1 transition, the low-energy shoulder in the preedge spectra (Figure 2) becomes weaker and the spectrum can be fitted with two strong components (~6541.1 and ~6542.8 eV) in the S_1 to S_3 states. Note that the instrumental resolution for the PS II RIXS data in Figure 1 is lower compared to that of the model compounds because the data were recorded at different experimental stations. However, the striking observation upon comparison of the PS II and model compound data is that the spectral changes during the PS II catalytic cycle (Figure 1) are considerably weaker than the spectral differences among the Mn^{IV} coordination complexes.

In the S_0 state, two different formal oxidation states, II,III,IV_2 and III_3,IV, have been proposed from the previous EPR,[10] X-ray absorption near-edge structure,[5] and other studies. Recent ^{55}Mn ENDOR studies[3] have shown that the data are compatible with the formal oxidation state of III_3,IV. In RIXS, Mn^{II} compounds show a characteristic feature due to the strong stabilizing energy of a $3d^5$ ^{5}S valence-shell configuration at around ~6540 eV. Unlike Mn^{IV} model compounds, Mn^{II} in both the oxide ($Mn^{II}O$; Figure 1a) and coordination complexes (not shown here) have very similar spectral features.[7] In the S_0 state, both RIXS and XAS data show spectral intensity at low energies (~6540 eV), which could indicate a contribution of Mn^{II}. This low-energy component becomes weak in the S_0 to S_1 transition. However, Mn^{III} compounds may also show a low-energy feature around ~6540 eV that originates from strong (3d, 3d) electron−electron interactions.[7] Therefore, a comparison of the RIXS S_0 spectrum with $Mn^{II}O$ (Figure 1a) does not confirm the presence or absence of Mn^{II} in the S_0 state.

A comparison of the S_3 RIXS spectrum with a series of Mn^{IV} coordination compound spectra suggests that the electronic structure of Mn in the S_3 state is much more similar to $salpn_2Mn_2^{IV}(OH)_2$ (Figure 1b) rather than $salpn_2Mn_2^{IV}O_2$ (Figure 1d), $phen_4Mn_2^{IV}O_2$ (Figure 1e), $Mn_3^{IV}O_4$Acbpy (Figure 1g), or the oxide $Mn^{IV}O_2$ (Figure 1h).

The OEC goes through four redox states during the S_0 to S_3 transitions. Our study shows that the RIXS spectral changes in PS II are considerably weaker than the changes observed within the Mn^{IV} coordination complexes. They are also weaker than the spectral changes between manganese oxides.[7] We, therefore, conclude that redox reactions of the OEC must be considered within the entire Mn_4CaO_5 entity. Namely, the ligands participate in the charge balancing. A description of the electronic structure at the Mn sites thus has to go beyond the assignment of formal oxidation states. We note that this does not contradict other studies such as EPR and ENDOR because a different response is probed in the various techniques.

We have shown that the formal oxidation states may be insufficient for describing the complex nature of the electronic structure in multinuclear clusters like the Mn_4CaO_5 cluster in PS II. Electrons are strongly delocalized in the Mn_4CaO_5 cluster, and ligands may be intimately involved in the redox chemistry. As a consequence, the Mn RIXS spectral changes are subtle during the *S*-state transitions. Of the two main mechanisms that are being considered for the O−O bond formation catalyzed by the OEC, one involves the generation of a Mn^V-oxo group in the final step when the O−O bond is formed, and the alternate mechanism involves delocalization of the charge onto a ligand and the subsequent chemistry of O−O bond formation.[6] The current results show that the change of the electronic charge includes the ligands in all *S*-state transitions. Therefore, the mechanisms that rely on delocalization of charge on the ligands may become more relevant, and any proposed mechanism requires one to take this into account. Such delocalization may play a role during the O−O bond formation step in the S_4 state.

■ ASSOCIATED CONTENT

Ⓢ Supporting Information

Materials and methods. This material is available free of charge via the Internet at http://pubs.acs.org.

■ AUTHOR INFORMATION

Corresponding Author

*E-mail: pieter.glatzel@esrf.fr, vkyachandra@lbl.gov, bergmann@slac.stanford.edu, jyano@lbl.gov.

Present Addresses

[§]Department of Physics, Purdue University, 525 Northwestern, West Lafayette, Indiana 47907.

[∞]Helmholtz-Zentrum-Berlin für Materialien und Energie GmbH, Hahn-Meitner-Platz D-14109 Berlin.

Notes

The authors declare no competing financial interest.

■ ACKNOWLEDGMENTS

This work was supported by NIH Grant GM 55302 and the DOE, Director, Office of Science, Office of Basic Energy Sciences (OBES), Chemical Sciences, Geosciences, and Biosciences Division, under Contract DE-AC02-05CH11231. Parts of this research were carried out at ESRF, APS, and SSRL operated by Stanford University for DOE, OBES. We thank Dr. Sumit Bhaduri for providing model complexes.

■ REFERENCES

(1) Wydrzynski, T.; Satoh, S. *Photosystem II: The Light-Driven Water:Plastoquinone Oxidoreductase*; Springer: Dordrecht, The Netherlands, 2005.

(2) Messinger, J. *Phys. Chem. Chem. Phys.* **2004**, *6*, 4764−4771.

(3) (a) Kulik, L. V.; Epel, B.; Lubitz, W.; Messinger, J. *J. Am. Chem. Soc.* **2005**, *127*, 2392−2393. (b) Kulik, L. V.; Epel, B.; Lubitz, W.; Messinger, J. *J. Am. Chem. Soc.* **2007**, *129*, 13421−13435.

(4) Iuzzolino, L.; Dittmer, J.; Dörner, W.; Meyer-Klaucke, W.; Dau, H. *Biochemistry* **1998**, *37*, 17112−17119.

(5) Messinger, J.; Robblee, J. H.; Bergmann, U.; Fernandez, C.; Glatzel, P.; Visser, H.; Cinco, R. M.; McFarlane, K. L.; Bellacchio, E.; Pizarro, S. A.; Cramer, S. P.; Sauer, K.; Klein, M. P.; Yachandra, V. K. *J. Am. Chem. Soc.* **2001**, *123*, 7804−7820.

(6) (a) McEvoy, J. P.; Brudvig, G. W. *Chem. Rev.* **2006**, *106*, 4455−4483. (b) Siegbahn, P. E. M. *Acc. Chem. Res.* **2009**, *42*, 1871−1880. (c) Yamanaka, S.; Isobe, H.; Kanda, K.; Saito, T.; Umena, Y.; Kawakami, K.; Shen, J. R.; Kamiya, N.; Okumura, M.; Nakamura, H.; Yamaguchi, K. *Chem. Phys. Lett.* **2011**, *511*, 138−145.

(7) Glatzel, P.; Bergmann, U.; Yano, J.; Visser, H.; Robblee, J. H.; Gu, W. W.; de Groot, F. M. F.; Christou, G.; Pecoraro, V. L.; Cramer, S. P.; Yachandra, V. K. *J. Am. Chem. Soc.* **2004**, *126*, 9946−9959.

(8) (a) Westre, T. E.; Kennepohl, P.; DeWitt, J. G.; Hedman, B.; Hodgson, K. O.; Solomon, E. I. *J. Am. Chem. Soc.* **1997**, *119*, 6297−6314. (b) de Groot, F.; Vanko, G.; Glatzel, P. *J. Phys.: Condens. Matter* **2009**, 21.

(9) (a) Baldwin, M. J.; Stemmler, T. L.; Riggsgelasco, P. J.; Kirk, M. L.; Pennerhahn, J. E.; Pecoraro, V. L. *J. Am. Chem. Soc.* **1994**, *116*, 11349−11356. (b) Mukherjee, S.; Stull, J. A.; Yano, J.; Stamatatos, T. C.; Pringouri, K.; Stich, T. A.; Abboud, K. A.; Britt, R. D.; Yachandra, V. K.; Christou, G. *Proc. Natl. Acad. Sci. U.S.A.* **2012**, *109*, 2257−2262.

(10) Messinger, J.; Robblee, J. H.; Yu, W. O.; Sauer, K.; Yachandra, V. K.; Klein, M. P. *J. Am. Chem. Soc.* **1997**, *119*, 11349−11350.